Structural and Enzymatic Studies of a New Analogue of Coenzyme B_{12} with an α-Adenosyl Upper Axial Ligand†

Kenneth L. Brown,*,‡ Shifa Cheng,‡ Xiang Zou,‡ Jing Li,‡ Guodong Chen,‡ Edward J. Valente,§ Jeffrey D. Zubkowski,|| and Helder M. Marques*,⊥

Department of Chemistry, Ohio University, Athens, Ohio 45701, Department of Chemistry, Mississippi College, Clinton, Mississippi 39085, Department of Chemistry, Jackson State University, Jackson, Mississippi 39217, and Centre for Molecular Design, Department of Chemistry, University of the Witwatersrand, P.O. Wits, 2050 Johannesburg, South Africa

Received March 27, 1998

ABSTRACT: A new analogue of coenzyme B_{12} (5′-deoxyadenosylcobalamin, AdoCbl), in which the configuration of the *N*-glycosidic bond in the Ado ligand is inverted [(α-ribo)AdoCbl], has been synthesized and its crystal structure determined by X-ray diffraction [MoK_α, $\lambda = 0.71073$ Å, monoclinic $P2_12_12_1$, $a = 16.132(12)$ Å, $b = 21.684(15)$ Å, $c = 27.30(3)$ Å, 9611 independent reflections, $R_1 = 0.0708$]. As suggested by molecular mechanics modeling before the structure was known, the Ado ligand lies over the southern quadrant of the molecule, as is the case for AdoCbl. The most striking feature of the structure is disorder in the orientation of the adenine (Ade) moiety relative to the ribose of the Ado ligand. This was resolved with a two-state model in which in the major (0.57 occupancy) conformer the A16(O)−A11−A9(N)−A8 dihedral angle is 1.9° and the Ade is virtually perpendicular to the corrin ring; in the minor conformer, the Ade is tilted down, and this dihedral is −48.7°. The Co−C and axial Co−N bond lengths and the Co−C−C bond angle are quite similar to those in AdoCbl. The corrin ring is considerably flatter than that of AdoCbl, with a fold angle of 11.7°. The molecule was successfully modeled by molecular mechanics (MM), and rotation of the Ado ligand relative to the corrin gave rise to four locally minimum structures with the Ado in the southern, eastern, northern, or western quadrant, with the southern conformation as the global minimum, as is the case with AdoCbl itself. Nuclear Overhauser effects (nOe's) observed by two-dimensional (2D) NMR were incorporated as restraints in molecular dynamics (MD) and simulated annealing (SA) calculations. A MD simulation at 300 K showed that only the southern conformation is populated with the Ado ligand confined to an arc from over C15 to over C12, while the Ade ring oscillates from perpendicular to parallel to the corrin ring. Twenty-seven structures were collected by MD−SA. Most of these annealed into the southern conformation, but examples of the other conformations were also found. The new analogue is a partially active coenzyme for the ribonucleotide reductase from *Lactobacillus leichmanii* with maximal activity that is 9.7% of that of AdoCbl itself, and a very high K_m value (245 μM compared to 0.54 μM for AdoCbl). In addition, the rate constant for enzyme-induced carbon−cobalt bond cleavage of (α-ribo)AdoCbl is 160-fold smaller than that for AdoCbl, and only $^1/_3$ as much cob(II)alamin is produced at the active site.

The 5′-deoxyadenosylcobalamin (AdoCbl[1])-requiring enzymes catalyze a series of intramolecular 1,2-rearrangements or the reduction of ribonucleotides to deoxyribonucleotides. The initial enzymatic step in each case is the cleavage of the carbon−cobalt bond of the coenzyme, a reaction catalyzed by these enzymes by as much as 10^{12}-fold (*1*−*4*). While the mechanisms by which these enzymes achieve this catalysis are not at all clear, distortion of AdoCbl by the enzyme is thought to play a role (*5*−*7*). However, it has been difficult to relate the well-known structure of AdoCbl (*8*−*13*) to its coenzymic function.

The structure of AdoCbl is somewhat peculiar with respect to the disposition and conformation of the adenosyl ligand (Figure 1). While the ribose ring is deployed perpendicular to the corrin ring, the adenine moiety is orthogonal to it,

† Supported by the National Institute of General Medical Sciences (Grant GM 48858 to K.L.B.), the Foundation for Research Development, Pretoria, South Africa (H.M.M.), and the University of the Witwatersrand.

* Address correspondence to these authors. K.L.B., phone, (740) 593-9465; fax, (740) 593-0148; e-mail, brownk3@oak.cats.ohiou.edu. H.M.M., phone, +2711-716-2303; fax, +2711-339-7967; e-mail, HMARQUES@AURUM.CHEM.WITS.AC.ZA.

‡ Ohio University.

§ Mississippi College.

|| Jackson State University.

⊥ University of the Witwatersrand.

[1] Abbreviations: AdoCbl, 5′-deoxyadenosylcobalamin (coenzyme B_{12}); CNCbl, cyanocobalamin (vitamin B_{12}); H_2OCbl^+, aquacobalamin; Bzm, 5,6-dimethylbenzimidazole; Ade, adenine; RTPR, ribonucleotide triphosphate reductase; 2′,5′-dideoxy-AdoCbl, 2′,5′-dideoxyadenosylcobalamin; Ado-13-epiCbl, 5′-deoxyadenosyl-13-epiCbl; CN-13-epiCbl, cyano-13-epicobalamin; AdePrCbl, adeninylpropylcobalamin; (α-ribo)-AdoCbl, *Co*-*β*-[α-(D-ribofuranosyladenin)yl]cobalamin; α-adenosine, α-(D-ribofuranosyl)adenine; HMPA, hexamethylphosphoramide; HEPES, *N*-(2-hydroxyethyl)piperazine-*N*′-2-ethanesulfonic acid; TSP, trimethylsilylpropionate; DTT, dithiothreitol; MD, molecular dynamics; SA, simulated annealing.

S0006-2960(98)00707-7 CCC: $15.00
Published on Web 06/13/1998

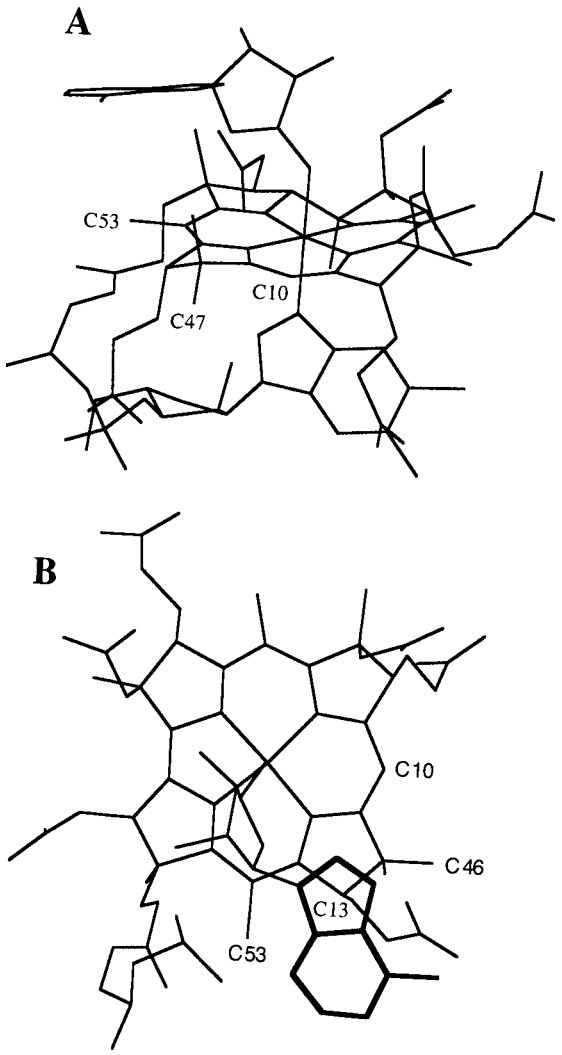

FIGURE 1: (A) Neutron diffraction structure of AdoCbl (*9*) viewed from the east, along the C10−Co axis. (B) Top view of the neutron diffraction structure of AdoCbl showing the southern conformation of the Ado moiety (the axial Bzm ligand has been removed for clarity).

and parallel to the corrin ring. Duplication of these features in structures modeled by molecular mechanics calculations (*14*−*16*) strongly suggests that these structural features are not the result of crystal-packing forces in the solid state. The conformation always found in the solid state (Figure 1) finds the purine in the southern quadrant, with its five-membered ring above corrin ring C13. This conformation is found to be the global energy minimum by molecular mechanics calculations (*14*−*16*), although rotation about the Co−C bond leads to three other local minima, one of which, with the adenine in the eastern quadrant, is known to be populated at room temperature from NMR studies (*16*, *17*). The northern and western conformations appear, from nOe measurements, to be populated at higher temperatures (*16*).

A number of structural analogues of AdoCbl (*18*−*29*), including some with modification in the Ado moiety itself (*21*, *22*, *26*, *27*), retain coenzymic activity with some enzymes,[2] albeit with reduced efficiency. Many other analogues are, however, inert. Structural studies of such analogues hold the promise of relating the well-known structural features of the coenzyme to its coenzymic function. A few such AdoCbl analogues have been studied by NMR,

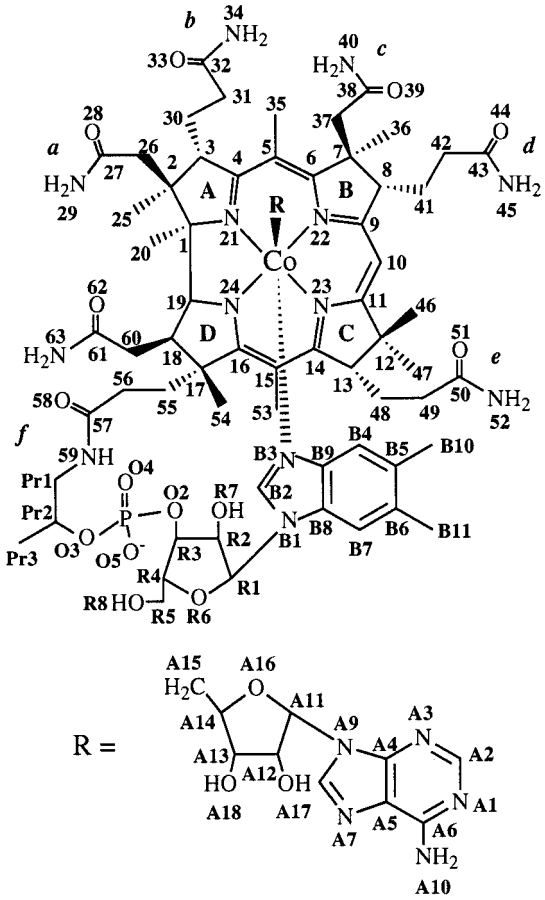

FIGURE 2: Numbering scheme for (α-ribo)AdoCbl.

including the [*ω*-(adenosin-5′-*O*-yl)alkyl]cobalamins (*30*), in which three to seven CH_2 groups are inserted between the cobalt atom and the 5′-oxygen of the Ado moiety, 2′,5′-dideoxy-AdoCbl (*31*), and Ado-13-epiCbl (*32*), and one such analogue has been studied by NMR and X-ray crystallography (*33*), namely, AdePrCbl, in which the ribose moiety of the Ado ligand is replaced by a propylene chain.

We now report the synthesis, characterization by X-ray crystallography, NMR, and NMR-restrained molecular modeling, and enzymology of a new structural analogue of AdoCbl in which the Ado ligand is an α-*N*-glycoside instead of the normal *β*-*N*-glycoside, abbreviated here as (α-ribo)-AdoCbl, the numbering scheme for which is shown in Figure 2. The synthesis and characterization of this analogue were undertaken to determine if the configuration of the *N*-glycosidic linkage in the Ado ligand was responsible for the particular conformation adopted by this ligand in AdoCbl. The α-diastereomer of adenosine, α-adenosine, is often found as a byproduct of the ribosylation of adenine, although several synthetic routes which favor this diastereomer have been devised (*34*−*36*). Interestingly, α-adenosine is a natural product, occurring as the lower axial nucleoside in the cobalt corrinoid factor C_x from *Propionibacterium shermanii* (*37*).

[2] AdoCbl-requiring enzymes appear to fall into two classes (W. Buckel, paper presented at the 4th European Symposium on Vitamin B_{12} and B_{12}-Proteins, September 2−6, 1996, Innsbruck, Austria), one of which (including the mutases, which catalyze carbon skeleton rearrangements) has much more stringent structural requirements for the coenzyme than the other (including diol dehydase and the B_{12}-requiring ribonucleotide reductases).

MATERIALS AND METHODS

Materials. α-Adenosine was from Sigma, and CNCbl was from Roussel. *Lactobacillus leichmannii* ribonucleotide triphosphate reductase (RTPR, EC 1.17.4.2) was obtained from transformed *Escherichia coli* HB101/PSQUIRE (*38*), the generous gift of J. Stubbe (Massachusetts Institute of Technology, Cambridge, MA), and purified to homogeneity as described (*38*). *E. coli* thioredoxin was from overproducing strain SK 3981 (*39*), and *E. coli* thioredoxin reductase was from overproducing strain K91/pMR14 (*40*).

5′-Chloro-5′-deoxy-α-adenosine. α-Adenosine (20 mg, 0.075 mmol) was dissolved in a mixture of 0.2 mL of HMPA and 0.040 mL of thionyl chloride and the mixture stirred overnight. Water (10 mL) was added, and the solution was loaded onto a small column of Dowex 50W-X8, H^+ form. The column was washed with 500 mL of water, and the product was eluted with a 1 M NH_4OH solution. The yield was 11.8 mg (55%).

(α-ribo)AdoCbl. CNCbl (132 mg, 0.097 mmol) was dissolved in 100 mL of a 10% (w/w) NH_4Cl solution, and the mixture was deaerated under a stream of argon for 60 min. An excess of zinc wool, briefly freshened with 1.0 M HCl, was added. 5′-Chloro-5′-deoxy-α-adenosine (11.8 mg, 0.041 mmol) in a deaerated aqueous solution was added via a cannula, and the reaction was allowed to proceed overnight under continuous argon purge. The reaction mixture was transferred to an aerobic 1.0 M HCl solution by cannula and desalted on a column of Amberlite XAD-2. The corrinoids were eluted with 50% (v/v) aqueous acetonitrile, and H_2OCbl^+ was removed by cation exchange chromatography on SP-Sephadex. The yield was 61.4 mg (95%) (based on a limiting 5′-chloro-5′-deoxy-α-adenosine concentration). The UV−visible spectrum was nearly identical to that of AdoCbl.

Enzyme Assays and Kinetics. UV−visible spectral measurements were taken on a Cary 3 spectrophotometer, the cell compartment of which was thermostated at 37 °C. The assay (*41*) mixture contained the following, in a 500 μL volume: 25 mM HEPES (pH 7.5), 4.0 mM EDTA, 1.0 mM dGTP, 2.0 mM ATP, 200 μM NADPH, 20 μM thioredoxin, 150 nM thioredoxin reductase, and 100−500 nM RTPR. The reaction was initiated by addition of 8 μM AdoCbl and monitored by the decrease in NADPH absorbance at 340 nm, using a $\Delta\epsilon_{340}$ of 6220 M^{-1} cm^{-1}, after subtraction of the background (<10% of the observed activity). For kinetic determinations with (α-ribo)AdoCbl, the RTPR concentration was increased 5−10-fold as needed.

Stopped-flow measurements of the RTPR-induced formation of cob(II)alamin from AdoCbl and (α-ribo)AdoCbl were taken at 525 nm in an Applied Photophysics SX.17MV stopped-flow spectrophotometer equipped with an AN1 anaerobic accessory. The light path was 1.0 cm long, and the dead time was about 1.8 ms. The sample unit was thermostated at 37.0 °C with a circulating water bath, and anaerobic conditions were maintained as described (*42*). One syringe contained enzyme, the allosteric effector dGTP, and DTT in 0.2 M sodium dimethylglutarate buffer (pH 7.3), and the other contained coenzyme and dGTP in the same buffer. After mixing, the final concentrations were 50 μM AdoCbl [or 100 μM (α-ribo)AdoCbl], 2 mM dGTP, 25 mM DTT, and 200 μM RTPR.

Table 1: Crystal Data for (α-ribo)AdoCbl

empirical formula	$C_{72}H_{100}CoN_{18}O_{17}P\cdot 19H_2O\cdot CH_3CN$
formula weight	1962.93
temperature (K)	294(2)
λ (MoKα) (Å)	0.71073
space group	$P2_12_12_1$
a (Å)	16.132(12)
b (Å)	21.6841(15)
c (Å)	27.30(3)
V (Å^3)	9551(14)
Z	4
crystal size (mm^3)	1.00 × 0.80 × 0.15
D (g cm^{-3})	1.327

X-ray Diffraction Analysis. Bright red crystals of (α-ribo)-AdoCbl were obtained by vapor phase diffusion of acetonitrile into an aqueous solution. A rod-like specimen (1.0 mm × 0.8 mm × 0.15 mm) was mounted in a glass capillary in contact with mother liquor. Measurements were taken on a Siemens P3 diffractometer in the dark. Preliminary examination with MoKα radiation revealed an orthorhombic system and space group $P2_12_12_1$. Abbreviated crystal data are given in Table 1, and complete data are given in the Supporting Information. Data were collected by Ω scans with a width of 2.0° with three standard reflections monitored after every 197 reflections. No deterioration was found over the course of the 147 h data collection period. A total of 10 155 reflections were collected, of which 9611 were unique, comprising a 0.995 complete octant to $2\theta = 47.5°$. The structure was solved by direct methods (*43*), and the full model was developed with difference Fourier calculations. Positions and anisotropic vibrational terms for non-H atoms (except for disordered atoms) were refined by full-matrix least-squares computations (*44*). Positions and anisotropic vibrational terms for non-H atoms of an acetonitrile and 17 ordered and two disordered waters were also found and included in the full model. H atoms were placed in calculated positions and allowed to ride on their attached non-H atoms. H atom isotropic vibrational factors were set to 120% of the equivalent isotropic vibrational factor for the attached non-H atom, except for the H atoms of the ribose hydroxyls, which were located and refined but with fixed isotropic vibrational factors. Adenine groups were found in two apparently disordered positions with considerable apparent vibrational motion perpendicular to the mean ring planes. Two orientations for the adenine were refined using a rigid group description from the X-ray structure of adenosine (*45*) in which the non-H atoms of the adenines were allowed to be refined with individual anisotropic vibrational terms. The final model converged with $R_1 = \sum||F_{obs}| - |F_{calc}||/\sum|F_{obs}| = 0.0708$ on F and $wR_2 = \{\sum[w(F_{obs}^2 - F_{calc}^2)^2]/\sum[w(F_{obs}^2)^2]\}^{1/2} = 0.1633$ on F_2 for $F > 2\sigma_F$. Heavy atom atomic coordinates, anisotropic displacement factors, hydrogen atom coordinates, an ORTEP drawing, a table of bond lengths and angles, and a description of hydrogen bonding contacts are available as Supporting Information.

NMR Spectroscopy. The sample (0.5 mL) was 20 mM in (α-ribo)AdoCbl and contained TSP as an internal reference in 90% H_2O/10% D_2O. Spectra were measured on a Varian Unity Inova 500 MHz NMR spectrometer equipped with pulsed field gradients. Two-dimensional homonulcear [TOCSY and ROESY (rotating frame Overhauser enhancement spectroscopy)] experiments with Watergate solvent suppres-

sion and heteronuclear (HMQC and HMBC) experiments were carried out as described previously (*32*). The ROESY spectra were obtained with mixing times of 50, 100, 150, and 200 ms, to classify the relative strengths of the observed nOe's.

Molecular Modeling. All energy minimizations and molecular dynamics (MD) and simulated annealing (SA) calculations were performed using HYPERCHEM version 4.5 or version 5.0,[3] the potential energy functions of the MM2 force field (*46*) (MM+ in HYPERCHEM), and the parameters we have derived for modeling the cobalt corrins (*14*−*16*). Additional information regarding the potential energy functions used is given as Supporting Information. The crystal structures of AdoCbl (*9*) and (α-ribo)AdoCbl were used as the starting point for modeling. Hydrogen atoms were placed in standard positions using ALCHEMY III.[4] A set of parabolic potential functions of the form $U_{nOe}(r_{ij}) = k_{nOe}(r_{ij} - r^{\circ}_{ij})^2$ were added to simulate the interproton distances, r_{ij}, determined from the two-dimensional (2D) ROESY spectra. On the basis of Clore et al. (*47*), the restraining force constant, k_{nOe}, was defined as $k_B TS/2(\Delta^{\pm}_{ij})^2$, where k_B is Boltzman's constant, T the absolute temperature, S a scaling factor, and $\Delta^{\pm}_{ij}$ the positive and negative error estimates of r_{ij}. We took S to equal 1, T to equal 300 K, and Δ^{+}_{ij} to equal Δ^{-}_{ij}. Nuclear Overhauser effect cross-peaks were classified as strong, medium, weak, or very weak (*48*−*51*) depending on whether they first appeared in the ROESY spectra at mixing times of 50, 100, 150, or 200 ms, respectively. Strong, medium, and weak nOe's are expected (*47*) when $r_{ij} < 2.7$ Å, 2.7 Å $< r_{ij} <$ 3.4 Å, and 3.4 Å $< r_{ij} <$ 4.0 Å, respectively. We set r°_{ij} equal to 2.5, 3.0, 4.0, and 4.5 Å and $\Delta^{\pm}_{ij}$ equal to 0.5, 0.75, 1.0, and 2.0 Å for strong, medium, weak, and very weak nOe's, respectively, giving k_{nOe} values of 1.2, 0.52, 0.3, and 0.075 kcal mol^{-1} Å^{-2} at 300 K for the four classes of nOe's. Violations of interproton distance restraints were taken as $r^{\circ}_{ij} + \Delta^{\pm}_{ij}$ for strong and medium nOe's (i.e., at 3.0 and 3.8 Å, respectively) and more stringently as r°_{ij} + 0.8 Å for weak and very weak nOe's (i.e., at 4.8 and 5.3 Å, respectively) since an nOe becomes essentially undetectable when $r_{ij} >$ ca. 5.0 Å (*46*). Prochiral protons were assigned on a trial and error basis until the minimum number of violations were obtained during a 25 ps MD simulation at 300 K.

For MD simulations, the leapfrog algorithm (*52*, *53*) was used to solve the classical Newtonian equations of motion and describe the dynamics trajectory. A small time step (0.5 or 1.0 fs) was used to allow integration of the highest-frequency motions of the system, usually C−H bond stretching vibrations. The temperature of the MD simulations was controlled by temperature scaling using coupling to an external heat sink (*54*) with a temperature relaxation time of 0.1 ps.

A typical MD simulation began with the assignment of velocities using a random number generator to a fully energy-minimized structure (rms gradient < 0.05 kcal Å^{-1} mol^{-1}). The molecule was then subjected to a 5 ps heating phase from 0 K to the desired run temperature (300 or 1000 K). For simulations designed to find stable conformations, the run phase varied between 0.1 and 25 ps. To explore interproton distances at room temperature, a run phase of 50 to 200 ps was used. For simulations designed to discover stable conformations, the run phase was followed by a cooling phase from the run temperature to 300 K.

[3] Hyperchem Inc., Gainseville, FL.
[4] Tripos Associates, St. Louis, MO.

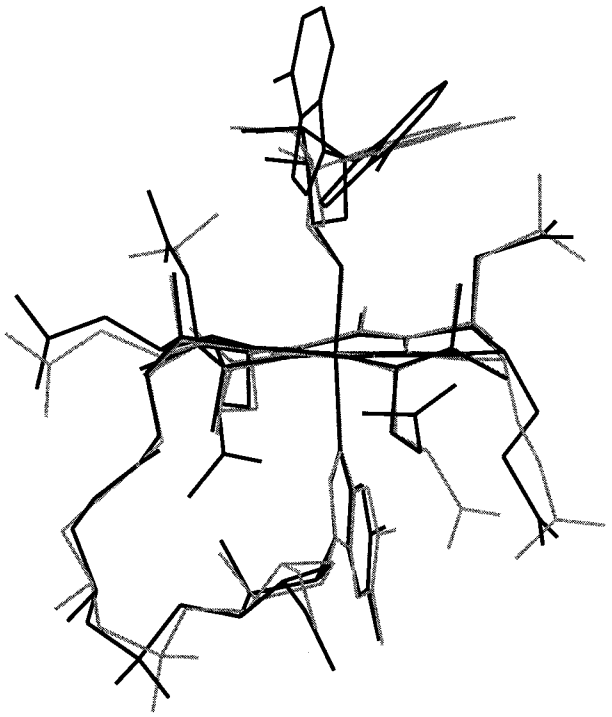

FIGURE 3: Superposition (at the four equatorial nitrogens) of the crystal structure of (α-ribo)AdoCbl (dark line, both conformers) and the crystal structure of AdoCbl (light line; *9*).

RESULTS

Preliminary Molecular Modeling. Before the synthesis of (α-ribo)AdoCbl was attempted, this diastereomer of AdoCbl was modeled to gauge its stability and, hence, the feasibility of its synthesis. Starting from the coordinates for the neutron diffraction structure of AdoCbl (*9*), we epimerized the structure at the *N*-glycosidic bond of the Ado ligand and then the N24−Co−A15−A14 dihedral angle, ω_1, was driven in 5° steps in both a clockwise and counterclockwise direction, with full energy minimization at each value of ω_1. A plot of the relative strain energy versus ω_1 (not shown) identified four local minima, in which the Ado ligand was over the southern, eastern, northern, or western quadrants of the corrin, as is the case for AdoCbl itself (*14*−*16*). The global minimum had the Ado in the southern conformation, as in AdoCbl, and the total strain energy was only 2.3 kcal mol^{-1} greater than that for the southern conformation of AdoCbl. This suggested that (α-ribo)AdoCbl would be stable, and indeed, its synthesis from 5′-chloro-5′-deoxy-α-adenosine was found to proceed with a nearly quantitative yield (95%).

X-ray Crystal Structure of (α-ribo)AdoCbl. As surmised from the molecular modeling, the crystal structure of (α-ribo)AdoCbl has the Ado ligand over the southern quadrant of the corrin. The most surprising result from the X-ray crystal structure is the finding of marked disorder in the adenosine group. Two principal conformations, differing primarily in the ribosidic torsion angles A16(O)−A11−A9(N)−A8, A16(O)−A11−A9(N)−A4, A12−A11−A9(N)−A8, and A12−A11−A9(N)−A4 could be modeled (Figure 3). In the

major conformation (0.57 occupancy), the A16(O)−A11−A9(N)−A8 torsion is 1.9° and the adenine ring is nearly perpendicular to the corrin. In the minor conformation, this torsion is −48.8° and the adenine is tilted downward, about halfway between its position in the major conformer and that in AdoCbl. This disorder is attended by considerable vibrational components that are perpendicular to the adenine rings of both conformers, but somewhat larger in the minor conformer. Plausible and roughly equivalent hydrogen bonding to the acceptor nitrogens (A1, A3, and A7) and the donor nitrogen (A10) is present for each conformer. H bonding from an A10 of the minor conformer is satisfied by an acceptor A3 of a major conformer in the neighboring molecule, whereas the A18 oxygen of the major conformer forms a H bond with an A1 acceptor of a neighboring major conformer. Partial occupancy water molecules in the vicinity of these donors and acceptors supply the necessary contacts with A10 and A18 when the adenine of the neighbor is in the alternate conformation.

It is clear from the displacement ellipsoids of the ribose ring atoms that the disorder is associated with conformational flexibility or static disorder in the adenosine ribose moiety as well. Two positions for the A17 oxygen could be modeled, and again, the vibrational motion evident in the minor conformer was larger than that for the major conformer. Other ribose atoms, including A11, A12, and the A16 oxygen, are probably disordered as well. However, models including this disorder show that a static representation would involve differences in their respective positions by less than half the resolution of the data (0.8 Å), and hence, the final model includes these atoms only with individual, anisotropic descriptions.

In the final model, the adenine ring is, of course, trans to A15 in the α-configuration. The average conformer of the ribose is in the C3-endo conformation, with A13 0.45 Å above and A12 0.18 Å below the plane described by A11, A14, and A16(O). This is quite similar to the adenosyl ribose conformation in the neutron diffraction structure of AdoCbl (*9*), where the ribose is also C3-endo, with A13 0.64 Å above and A12 0.12 Å below the A11−A14−A16(O) plane.

The overall structure of the Cbl moiety in (α-ribo)AdoCbl is quite similar to that of AdoCbl (Figure 3), although there are differences in side chain conformations, and the corrin ring fold angle (*55*), 11.7°, is smaller than that of AdoCbl (14.6°), indicating a "flatter" corrin ring. The inner sphere geometry (Table 2) is somewhat distorted, with the Co−N21 and Co−N23 bonds slightly shorter and the Co−N22 and Co−N24 bonds slightly longer than those in AdoCbl. The axial bond lengths are, however, quite similar, as are the inner sphere and Co−C−C bond angles.

Post-X-ray Molecular Modeling. Beginning from the coordinates of the major component of the crystal structure of (α-ribo)AdoCbl, we reproduced the structure reasonably well with molecular mechanics modeling (Figure 4), although the orientation of the Ado ligand is somewhat different. The N24−Co−A15−A14 torsion angle, ω_1, is 26.9° in the crystal structure but 52.1° in the modeled structure, so the Ado ligand is rotated somewhat counterclockwise. However, the C3-endo conformation of the ribose is preserved in the modeled structure, and the disposition of the adenine ring relative to the ribose is the same as that of the minor conformation of the crystal structure, the A16(O)−A11−A9(N)−A8 torsion angles being −48.8° in the crystal structure and −48.5° in the modeled structure. The coordination sphere is also well preserved in the modeled structure (Table 2), although the Co−N21 and Co−N23 bonds are somewhat longer and the Co−N22 and Co−B3-(N) bonds are somewhat shorter in the modeled structure. The corrin ring fold angle in the modeled structure, 11.0°, duplicates that of the crystal structure (11.7°) very closely.

Table 2: Comparison of the Inner Sphere Geometry of the Crystal Structures of (α-ribo)AdoCbl and AdoCbl and the Molecular Mechanics Structure of (α-ribo)AdoCbl

	(α-ribo)AdoCbl (X-ray)	AdoCbl (X-ray)[a]	(α-ribo)AdoCbl (MM)[b]
	Bond Lengths (Å)		
Co−A15(C)	2.016(11)	1.999	2.027
Co−B3(N)	2.238(10)	2.237	2.181
Co−N21	1.838(10)	1.873	1.897
Co−N22	1.975(10)	1.906	1.940
Co−N23	1.871(11)	1.905	1.935
Co−N24	1.904(10)	1.886	1.900
	Bond Angles (deg)		
A15(C)−Co−B3(N)	173.2(4)	172.7	172.5
A15(C)−Co−N21	90.1(5)	92.5	92.5
A15(C)−Co−N22	83.6(4)	84.3	86.1
A15(C)−Co−N23	94.4(5)	92.2	89.8
A15(C)−Co−N24	93.3(4)	92.5	90.4
B3(N)−Co−N21	91.6(4)	90.7	92.7
B3(N)−Co−N22	89.8(4)	89.1	88.4
B3(N)−Co−N23	84.6(4)	85.4	85.6
B3(N)−Co−N24	93.4(4)	94.5	95.6
Co−A15(C)−A14(C)	124.9(9)	124.4	122.4

[a] Ref *9*. [b] Molecular mechanics model. See the text.

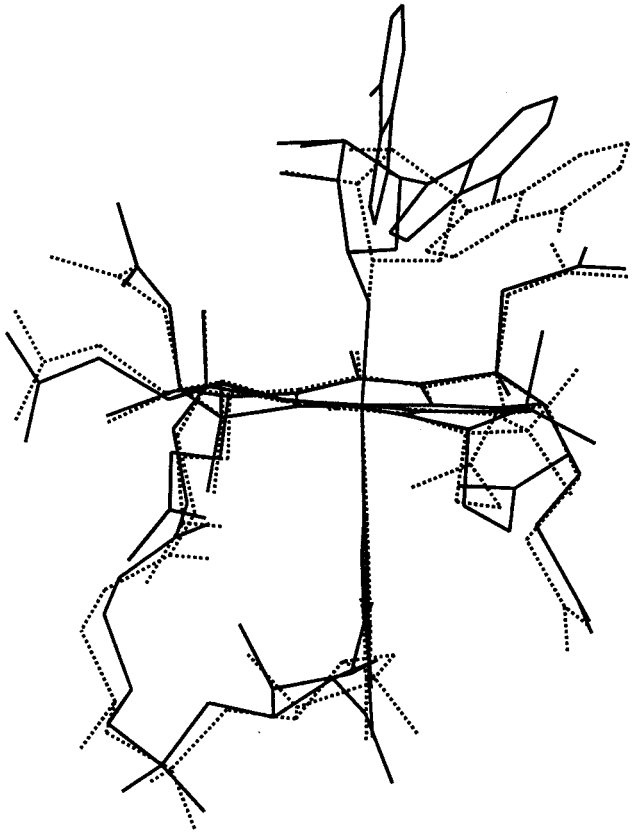

FIGURE 4: Superposition (at the four equatorial nitrogens) of the crystal structure of (α-ribo)AdoCbl (solid line) and the molecular mechanics structure (dotted line) obtained by starting from the coordinates of the major component of the crystal structure.

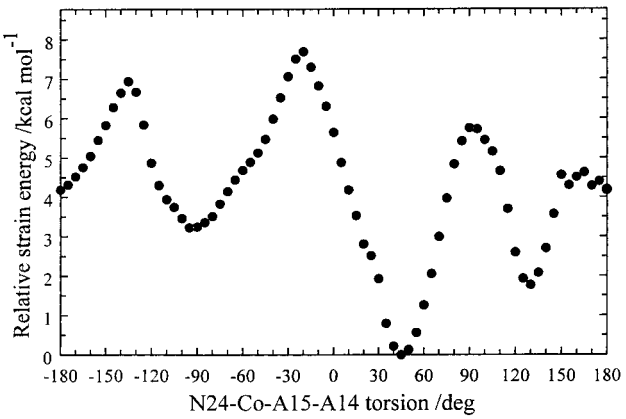

FIGURE 5: Strain energy as a function of rotation of the Ado ligand of (α-ribo)AdoCbl about the Co−C bond.

Table 3: Selected ^{13}C NMR Chemical Shifts of (α-ribo)AdoCbl and AdoCbl

	chemical shift (ppm)			
atom	(α-ribo)AdoCbl	AdoCbl[a]	$\Delta\delta_{^{13}C}$[b] (Cbl)	$\Delta\delta_{^{13}C}$ (adenosine)[c]
C15	105.78	106.70	−0.92	
C46	33.38	33.84	−0.46	
C47	24.28	23.59	0.69	
C48	29.33	29.98	−0.65	
A5	120.50	121.51	−1.01	−1.2
A11[d]	85.81	90.57	−4.76	−2.9
A12[e]	72.61	75.14	−2.53	−2.8
A13	76.98	76.15	0.87	0.1
A14[f]	87.20	88.19	−0.99	−2.0
A15	27.71	26.95	0.76	−0.1

[a] Ref *59*. [b] $\Delta\delta = \delta_{(\alpha-\text{ribo})\text{AdoCbl}} - \delta_{\text{AdoCbl}}$. [c] $\Delta\delta = \delta_{\alpha-\text{adenosine}} - \delta_{\beta-\text{adenosine}}$ (*60*). [d] $\Delta\delta^1_H = 0.48$ ppm. [e] $\Delta\delta^1_H = -0.25$ ppm. [f] $\Delta\delta^1_H = 0.19$ ppm.

The strain energy profile for rotation of the Ado ligand about the Co−C bond was reinvestigated, starting from the MM structure shown in Figure 4. The results (Figure 5) confirm the existence of four local minima, with the southern conformation being the global minimum. Interestingly, the energy barriers for rotation from the southern conformation are much higher than those for AdoCbl itself, where the eastern conformation is accessible and populated at room temperature (*16*, *17*) and the northern and western conformations are probably populated at 60 °C (*16*).

NMR Spectra of (α-ribo)AdoCbl. The ^{1}H and ^{13}C NMR spectra of (α-ribo)AdoCbl in aqueous solution were completely assigned using the now standard battery of homonuclear and heteronuclear 2D NMR experiments and assignment strategies (*17*, *56*−*58*). A NMR correlation table and the ^{1}H and ^{13}C assignments are available as Supporting Information. The only significant differences in ^{13}C chemical shifts from AdoCbl (*56*, *59*) occurred in the Ado ligand, at corrin ring C15, and at peripheral carbons C46, C47, and C48. The chemical shifts for these carbons in (α-ribo)-AdoCbl and AdoCbl, along with the difference in chemical shift between the two compounds, are shown in Table 3. Also shown in Table 3 are the differences in ^{13}C chemical shifts between α-adenosine and the normal β-diastereomer of adenosine (*60*). All of the Ado carbons of (α-ribo)AdoCbl have significant chemical shift differences upon epimerization of the Ado *N*-glycoside except A2, A4, and A6. However, it is clear from the comparison of α- and β-adenosine that there are chemical shift differences between the Ado ligand of (α-ribo)AdoCbl and AdoCbl which cannot be attributed to the change of configuration at the *N*-glycosidic bond alone (i.e., A11, A13, A14, and A15).

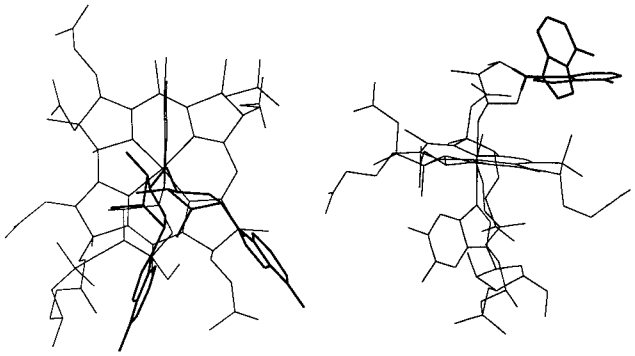

FIGURE 6: Motion of the Ado ligand during a 300 ps NMR-restrained molecular dynamics simulation of (α-ribo)AdoCbl at 300 K. The orientations shown are the extremes of motion observed.

In the rotating frame Overhauser enhancement (ROESY) spectrum measured at the longest mixing time (200 ms), 113 assignable nOe cross-peaks (not including those due to geminal hydrogens) were resolved at 500 MHz, including 11 between Ado and non-Ado hydrogens. A complete listing of these nOe's and their strengths is available as Supporting Information.

NMR-Restrained Molecular Modeling. The observed nOe's, except for those between Ado and non-Ado protons, were incorporated as parabolic restraints into the molecular modeling. A 300 ps MD simulation (in steps of 0.5 fs) was run at 300 K, and all interproton distances were monitored. The minimum, maximum, mean, and standard deviation of these distances are given in the Supporting Information. Of the 102 nOe's monitored, only five (4.9%) violated the distance criteria on average. During this MD simulation, the N24−Co−A15−A14 dihedral angle, which describes the disposition of the Ado ligand relative to the corrin ring, and the A16(O)−A11−A9(N)−A8 dihedral angle, which describes the disposition of the adenine relative to the ribose, were also monitored. The former dihedral was confined to 12.0−69.6° (mean of 39.5 ± 8.4°, compared to 26.9° in the crystal structure), showing that only the southern conformation was populated at this temperature (Figure 6). The A16-(O)−A11−A9(N)−A8 dihedral varied from −77.2 to 25.6° (mean of −32.1 ± 14.5°, compared to 1.9 and −48.8° in the major and minor conformations of the crystal structure, respectively); i.e., the Ade moiety fluctuated from virtually parallel to nearly perpendicular to the corrin ring (Figure 6).

During this run, the interproton distances associated with the nOe's between Ado and non-Ado protons (which were not used as restraints) were also monitored. As seen in Table 4, all of these nOe's except the one between the C10(H) and A14(H) were compatible with their distance restraints, suggesting that these nOe's all arise from the observed southern conformation and that this is the only conformation populated at this temperature. Moreover, the mean H−H distance tends to increase as the observed nOe strength decreases (Table 4).

Twenty-seven annealed structures of (α-ribo)AdoCbl were obtained starting from the crystal coordinates and heating (5 ps, 300−1000 K), running at 1000 K for 0−25 ps, and

Table 4: Ado−Non-Ado H−H Distances for Observed nOe's during a 300 ps MD Simulation of (α-ribo)AdoCbl at 300 K

nOe	intensity[a]	min (Å)	max (Å)	mean (Å)	SD (Å)
A11(H)−C46(H_3)	S	1.998	4.522	3.350	0.402
A15(H′)−C37(H′)	M	3.737	6.034	5.032	0.312
A15(H′)−C19(H)	M	1.873	3.347	2.471	0.217
A8(H)−C54(H_3)	M	1.836	4.794	3.212	0.512
A8(H)−C53(H_3)	M	1.914	5.258	3.255	0.751
A15(H″)−C37(H″)	W	3.905	5.139	4.536	0.178
A14(H)−C46(H_3)	W	2.870	5.575	4.205	0.369
A15(H″)−C10(H)	VW	3.413	4.838	4.052	0.196
A14(H)−C10(H)	VW	5.193	6.852	6.068	0.246
A8(H)−C46(H_3)	VW	1.857	5.110	3.211	0.546
A8(H)−C13(H)	VW	1.939	5.031	3.058	0.514

[a] Strong (S), medium (M), weak (W), or very weak (VW) assigned for nOe cross-peaks which first appeared in the ROESY spectrum at 50, 100, 150, or 200 ms mixing times, respectively.

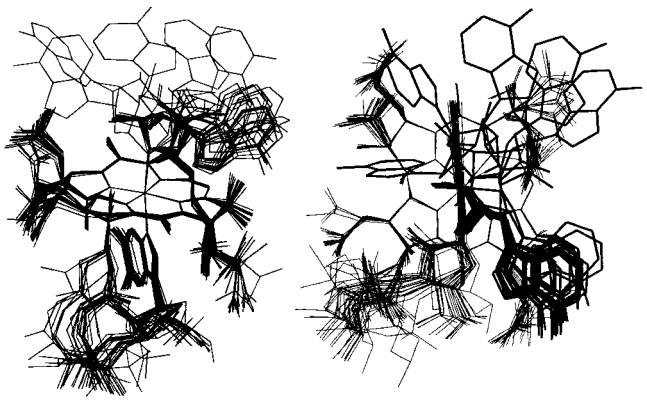

FIGURE 7: Overlay from two different perspectives of the 27 annealed structures of (α-ribo)AdoCbl.

then cooling to 300 K over the course of 10 ps, followed by full energy minimization. During this procedure, all nOe restraints were maintained except those between Ado and non-Ado protons to explore the conformational flexibility and preferences with respect to the disposition of the Ado ligand. Of the 27 structures, 21 annealed into the southern conformation, two into eastern to northeastern conformations, three into northern to northwestern conformations, and one into a western conformation (Figure 7).

The great majority of structures annealed with the nucleotide loop in the "inward" conformation, usually seen in the solid state, in which the C57−O58 carbonyl (viewed from above) points toward the southeast and the C57−O58 vector intersects the Co−C15 vector (Figure 2 of the Supporting Information). However, three structures annealed with the "outward" nucleotide loop conformation, seen in the X-ray crystal structure of 10-Cl-H_2OCbl$^+$ (*61*), in which the C57−O58 vector points to the southwest, away from the molecule. It seems likely that in solution the nucleotide loop side chain oscillates between these extremes, with the C57−O58 vector describing a broad arc.

The orientation of the C ring in the annealed structures is also of interest. C46 varies from a prominent axial position to a pseudoequatorial position (Figure 3 of the Supporting Information). Although the C46 axial position is the usual one seen in the solid state [including (α-ribo)AdoCbl], evidence of disorder in the C ring and the population of a C46 pseudoequatorial conformer was recently obtained with a series of C10 chloro-substituted cobalamins (*61*). These results suggest that this flexibility in the C ring may be more common than previously realized.

The *a* and *d* side chains in all 27 structures annealed into similar positions, but there was considerable variability in the final disposition of the others (Figure 4 of the Supporting Information). The *b* side chain occupied one of two sites, with the amide pointing to the α-face (lower) in one and to the β-face (upper) in the other. The *c* side chain is quite flexible, and the annealed structures virtually describe a cone. The *e* side chain also annealed into one of two positions, one with the amide pointing downward toward the α face and one with the amide parallel to the corrin. There is also considerable variability in the final orientation of the *g* side chain.

Coenzymic Activity of (α-ribo)AdoCbl. In the standard activity assay for RTPR using thioredoxin as the reducing agent, (α-ribo)AdoCbl supported a slow reduction of ATP to dATP. When the RTPR concentration was 10 times the normal concentration, the K_m value for (α-ribo)AdoCbl was determined to be 245 μM, compared to 0.54 μM for AdoCbl. The maximal activity that can be obtained with (α-ribo)-AdoCbl was 9.7% of the maximal activity with the natural coenzyme.

As reported previously by Tamao and Blakley (*62*) and by Licht et al. (*42*), RTPR-induced cleavage of the carbon−cobalt bond of AdoCbl could be monitored spectrophotometrically in an incomplete system consisting of the coenzyme, the enzyme, the allosteric effector dGTP, and a thiol reductant. At 525 nm, the wavelength of maximal spectral change for conversion of AdoCbl to cob(II)alamin, a rapid decrease in absorbance, complete in <100 ms and representing reversible formation of cob(II)alamin (*42*, *62*), is followed by a much slower decrease representing the irreversible decomposition of AdoCbl to cob(II)alamin and 5′-deoxyadenosine (*62*) (Figure 5A of the Supporting Information). Since the slower decrease is ca. 7000-fold slower than the rapid change, the data for the faster change could be successfully fitted to a single-exponential decay restricting the observations to the first 100 ms. We observed a rate constant of 42 s^{-1} at 37 °C using DTT as the thiol reductant, consistent with the value of 38 s^{-1} reported by Tamao and Blakley (*62*), who also used DTT, and with the value of 42 s^{-1} reported by Licht et al. (*42*), who used the physiological reducing system thioredoxin/thioredoxin reductase/NADPH. The slower spectral change, associated with the irreversible loss of coenzyme, was also first-order and had a rate constant of 6.1×10^{-3} s^{-1}.

A similar pattern of absorbance change was observed for (α-ribo)AdoCbl (Figure 5B of the Supporting Information), except that the absorbance change associated with the rapid formation of cob(II)alamin was smaller and the change much slower, although the slower absorbance change occurred on the same time scale as that for AdoCbl. The data were consequently fit to a double-exponential decay and gave rate constants of 0.26 s^{-1} for the fast spectral change and 8.8×10^{-3} s^{-1} for the slow change.

DISCUSSION

As is the case in all of the crystal structures of AdoCbl (*8*−*13*), (α-ribo)AdoCbl crystallizes with the Ado ligand in the southern conformation. This work strongly suggests that this is also the predominant, if not the only, conformation adopted in solution as well. Preliminary MM modeling

based on the X-ray coordinates of AdoCbl after epimerization at A11 correctly predicted that the southern conformation would be the most stable. Subsequent MM calculations based on the X-ray coordinates of (α-ribo)AdoCbl also confirm that the southern conformation is the most stable of four possible conformations (Figures 4 and 5). This situation is similar to that of AdoCbl itself (*14*−*16*), except that for AdoCbl, the barrier to rotation from the southern to the eastern conformation is much smaller, so the eastern conformation is populated as well at ordinary temperatures. In addition, the NMR-restrained MD simulation (Figure 6) shows the molecule existing in a range of conformations, in all of which the Ado ligand is well within the potential energy well defining the southern conformation (Figure 5). Also, all of the nOe's observed between protons on the Ado ligand and protons on the Cbl moiety, save one very weak nOe, were compatible with the southern conformation (Table 4), despite the fact that these nOe's were not used as distance restraints during the simulations. Importantly, the vast majority of the structures generated by nOe-restrained simulated annealing calculations (again, without imposing the Ado−non-Ado nOe restraints) had a southern conformation, confirming this conformation as the global minimum (Figure 7). Annealed structures with other conformations confirm the existence of the other local minima seen in the strain energy profile of rotation about the Co−C bond (Figure 5), but there is clearly no evidence that these other conformations are populated at ordinary temperatures.

For the other AdoCbl analogues which have been studied to date, Calafat et al. (*31*) inferred a southern conformation for 2′,5′-dideoxy-AdoCbl from nOe observations. However, in Ado-13-epiCbl, NMR and molecular modeling results suggest that the southern conformation cannot be adopted since epimerization at C13 places the *e* side chain in the region of space that would be occupied by the Ado ligand in this conformation. Instead, several conformations seem to be populated on the basis of nOe observations (*32*). In the only other analogue of AdoCbl which has been studied by X-ray crystallography, AdePrCbl (*33*), in which the ribose ring is replaced by a three-carbon alkyl chain, the adenine is rotated some 120° clockwise from its position in AdoCbl, occupying a western conformation.

The most striking aspect of the crystal structure of (α-ribo)AdoCbl is the disorder in the conformation of the Ado ligand, successfully modeled by two conformations in which the tilt of the adenine ring system relative to the ribose ring differs (Figure 3). Both conformations are significantly different from that displayed in the AdoCbl structure, but the minor conformer (0.43 occupancy) has an adenine tilt closer to that of AdoCbl. This disorder suggests that there is flexibility in the conformation of the Ado ligand of (α-ribo)AdoCbl and that more than one conformation with respect to the adenine tilt can be assumed.

There is clear evidence that the Ado conformation of (α-ribo)AdoCbl in solution is different from that of AdoCbl. The changes in ^{13}C chemical shift of the Ado moiety of AdoCbl upon epimerization at A11 are clearly different from those which occur upon epimerization of free adenosine (Table 3). This suggests that there are differences in the magnetic environment of the Ado ligand of (α-ribo)AdoCbl beyond those caused by the epimerization itself.

In addition, there are significant differences in ^{13}C chemical shift between (α-ribo)AdoCbl and AdoCbl at C15, C46, C47, and C48 (Table 3). All of these carbons are in the vicinity of the Ado ligand in the normal southern conformation of AdoCbl, and their chemical shifts thus may be affected by the magnetic anisotropy of the adenine (*63*). The upward tilting of the adenine in (α-ribo)AdoCbl might significantly reduce the anisotropic shielding of the carbons in this region, causing changes in chemical shift. Indeed, ^{1}H chemical shift differences at C46 and C13 between AdoCbl and AdePrCbl have been attributed to the change in position of the adenine in the latter complex (*33*). However, it is difficult to understand in the current case why the C12 and C13 carbon resonances would not also be affected.

An alternate possibility is that these chemical shifts are affected by the flexibility in the C ring detected by molecular modeling. In the 10-Cl-XCbl's (*61*), such flexibility, which causes disorder in this region of the corrin, has profound effects on ^{13}C chemical shifts, particularly those of the C46 and C47 methyls. In most Cbl's, these methyl resonances are separated by about 12 ppm due to differential steric effects of the neighboring *e* side chain on the upwardly axial C46 and the equatorial C47 (*59*). In CN-13-epiCbl, inversion of configuration at C13 reverses this steric effect and inverts the chemical shifts of the now equatorial C46 and the downwardly axial C47. In the 10-Cl-XCbl's, an apparent C ring flip leads to a decrease in the chemical shift difference between these two methyl of about 5 ppm (*61*). In (α-ribo)-AdoCbl, the C46 and C47 resonances are shifted in opposite directions from their positions in AdoCbl. The resulting decrease in chemical shift difference (ca. 1.1 ppm) could thus be due to C ring flexibility. However, this would also be expected to affect the chemical shifts of C12 and C13, so neither of these explanations for the ^{13}C chemical shift differences between (α-ribo)AdoCbl and AdoCbl seems to be completely compatible with the observations.

Most importantly, the nOe-restrained molecular dynamics simulation (Figure 6) strongly suggests that in solution the Ado ligand of (α-ribo)AdoCbl can adopt a wide range of conformations with respect to the tilt of the adenine ring relative to the ribose. These range from a conformation in which the adenine is essentially parallel to the corrin ring, as it is in AdoCbl, to one in which the adenine is nearly perpendicular to the corrin, as it is in the major conformer of the crystal structure of (α-ribo)AdoCbl.

The particular conformation of the Ado ligand in AdoCbl (Figure 1) can be understood by comparison to the crystal structures of adenosine and derivatives of adenosine substituted at the 5′-carbon (A15 in the AdoCbl numbering scheme). The tilt of the adenine relative to the ribose in adenosine derivatives is largely controlled by the dihedral angles A16(O)−A11−A9(N)−A8, A16(O)−A11−A9(N)−A4, A12−A11−A9(N)−A8, and A12−A11−A9(N)−A4. Values for these dihedral angles are given in Table 5 for adenosine and AdoCbl, as well as for adenosine 5′-*O*-methyl phosphate (*64*), adenosine 5′-*O*-diethyl phosphate (*65*), both conformers of the crystal structure of (α-ribo)AdoCbl, and the molecular mechanics model of (α-ribo)AdoCbl. The four dihedral angles are substantially different in adenosine and AdoCbl, leading to the conformational difference shown in Figure 8A, a superposition (at the ribose ring atoms) of the

Table 5: Values for Selected Dihedral Angles in AdoCbl, (α-ribo)AdoCbl, Adenosine, and Some 5′-Substituted Adenosines

	dihedral angle (deg)			
	A16(O)−A11−A9(N)−A8	A16(O)−A11−A9(N)−A4	A12−A11−A9(N)−A8	A12−A11−A9(N)−A4
adenosine[a]	9.9	−171.4	−108.6	70.1
AdoCbl[b]	69.8	−101.6	−49.6	139.0
adenosine 5′-*O*-methyl phosphate[c]	68.7	−113.5	−50.4	127.4
adenosine 5′-*O*-diethyl phosphate[d]	69.0	−107.7	−47.0	136.3
(α-ribo)AdoCbl (major conformer)[e]	1.9	175.7	117.1	−69.2
(α-ribo)AdoCbl (minor conformer)[f]	−48.7	136.6	83.8	−90.8
(α-ribo)AdoCbl (MM model)[g]	−48.5	131.4	68.4	−113.2

[a] Ref *45*. [b] Ref *9*. [c] Ref *64*. [d] Ref *65*. [e] This work (0.57 occupancy). [f] This work (0.43 occupancy). [g] Figure 4.

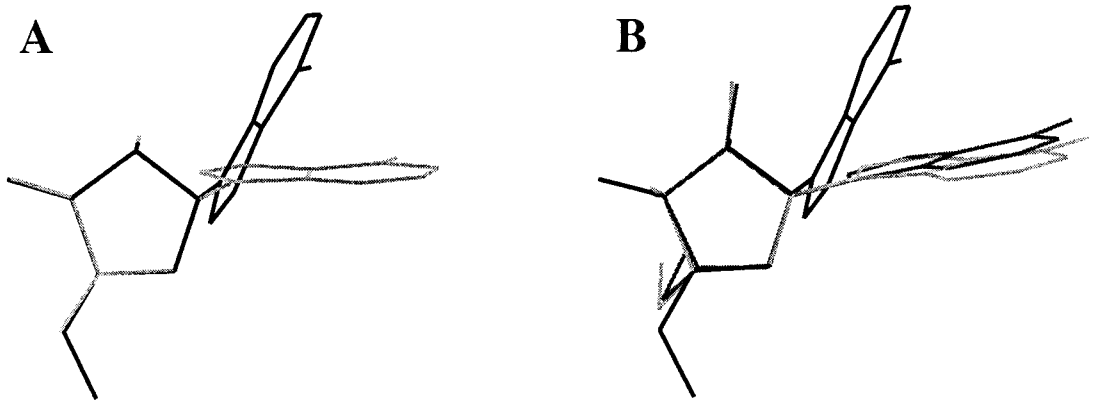

FIGURE 8: (A) Superposition (at the ribose ring atoms) of the crystal structure of adenosine (dark line) with the Ado moiety of AdoCbl (light line). (B) Superposition (at the ribose carbons) of the crystal structure of adenosine (dark line) with the Ado moiety of adenosine 5′-*O*-methyl phosphate (medium line) and adenosine 5′-*O*-diethyl phosphate (light line).

Ado moiety of AdoCbl with adenosine. Figure 8B shows a similar comparison of adenosine with the Ado moieties of the 5′-substituted derivatives, adenosine 5′-*O*-methyl phosphate and adenosine 5′-*O*-diethyl phosphate. It is clear that 5′-substitution results in a downward tilt of the adenine ring system (by about 60°) similar to that seen in AdoCbl, with the defining dihedral angles of the two substituted adenosines being very similar to those of AdoCbl (Table 5). Thus, substitution at the 5′-carbon of adenosine enforces a downward tilt of the adenine, presumably due to steric repulsion between the 5′-substituent and the adenine when both are on the same side of the ribose ring, even when the substituent is substantially smaller than cobalamin. Although no crystal structures are available for α-adenosine or any of its 5′-substituted derivatives, evidently when a 5′-substituent and the adenine are on opposite sides of the ribose ring, the greatly reduced steric interaction allows the adenosyl moiety to adopt less extreme conformations and allows for significant conformational flexibility. As seen in Table 5, the four defining dihedral angles in both conformers of (α-ribo)-AdoCbl are quite different from those in AdoCbl, and the molecular mechanics model of (α-ribo)AdoCbl closely resembles the minor conformer with respect to the adenine tilt.

Although it may be unusual for an optical isomer of a coenzyme to be biologically active, the low activity of (α-ribo)AdoCbl seems in some sense surprising. The Co−C bond length and Co−C−C bond angles, crucial determinants of the Co−C bond dissociation energy (*15*), of (α-ribo)-AdoCbl and AdoCbl are nearly identical (Table 2). Moreover, during the molecular dynamics simulation of (α-ribo)AdoCbl at 300 K (Figure 6), the Ado ligand clearly can adopt a conformation which is very similar to that of AdoCbl in the solid state. However, this assumes that the conformation of AdoCbl seen in the solid state is in fact the coenzymically active one, and it is currently not clear that this is the case.

In our recent study of Ado-13-epiCbl (*32*), we found that this coenzyme analogue is unable to adopt the southern conformation seen in the crystal structure of AdoCbl because epimerization at C13 places the *e* side chain in the region of space which would be occupied by the Ado ligand in a southern conformation. Yet Ado-13-epiCbl is a partially active coenzyme for diol dehydrase, with 14% of the activity of AdoCbl and a K_m value only 13-fold higher than that for AdoCbl (*20*). These observations force us to consider the possibility that it is the eastern conformation which is the active one, since this conformation is accessible to both AdoCbl and Ado-13-epiCbl at ordinary temperatures. However, our molecular mechanics calculations suggest that there is a relatively large energy barrier of 5−6 kcal mol^{-1} for rotation from the southern to the eastern conformation in (α-ribo)AdoCbl (Figure 5), and the NMR and molecular modeling results suggest that the eastern conformation is not populated at ordinary temperatures (although it is accessible at elevated temperatures as shown by the simulated annealing results). Consequently, if the eastern conformation is indeed the active one, the enzyme must use binding free energy to enforce this conformation on enzyme-bound (α-ribo)AdoCbl.

It is clear that proteins are capable of binding cobalamins extremely tightly, as seen in the affinity of B_{12} binding proteins for CNCbl (*66*−*68*) which, in the case of haptocorrin, can have binding constants as high as 5×10^{16} M^{-1}, representing nearly 23 kcal mol^{-1} of binding free energy (*68*). AdoCbl-requiring enzymes bind AdoCbl much less tightly, so significant binding free energy may well be available for

distorting the coenzyme, a process which may be an integral part of normal catalysis (vide infra). Our kinetic data for (α-ribo)AdoCbl with RTPR and Fersht's work on the thermodynamics of the association of ligands with enzymes (*69*−*71*) allow estimation of the loss of binding energy due to epimerization at the *N*-glycosidic bond in the coenzyme as $\Delta\Delta G_b = -RT \ln[(k_{cat}/K_m)_{(\alpha-ribo)AdoCbl}/(k_{cat}/K_m)_{AdoCbl}] = 5.1$ kcal mol^{-1}. This is approximately the amount of energy needed to surmount the energy barrier between the southern and eastern conformations (Figure 5) and enforce an eastern conformation on bound (α-ribo)AdoCbl. Thus, the possibility that the eastern conformation is in fact the active one remains real, despite the fact that there is no evidence that this conformation for (α-ribo)AdoCbl is populated at ordinary temperatures.

There are, of course, other possible explanations for the low activity and weak binding of (α-ribo)AdoCbl. Even though the analogue appears to be able to adopt a conformation very similar to that of AdoCbl during a molecular dynamics simulation, inversion about the *N*-glycoside may make it impossible for the Ado ligand to adopt an ideal conformation at the active site with respect to the spatial disposition of potential hydrogen bonding functionalities. If such hydrogen bonding to the Ado ligand is important in the binding of AdoCbl or its activation for Co−C bond cleavage, the complete loss of several (or the partial loss of even more) such hydrogen bonds could explain the observed decrease in binding energy.

Our kinetic results for the RTPR-induced cleavage of the carbon−cobalt bond of (α-ribo)AdoCbl are compatible with such an explanation. From the observed molar spectral change for the rapid reaction with AdoCbl, assuming that the coenzyme is completely bound in the presence of 200 μM RTPR and a value of 4800 M^{-1} cm^{-1} for the change in molar absorptivity at 525 nm for complete conversion of AdoCbl to cob(II)alamin (*42*), 0.3 equiv of cob(II)alamin per equivalent of enzyme is formed in the rapid reaction. For (α-ribo)AdoCbl, using 4670 M^{-1} cm^{-1} as the $\Delta\epsilon_{525}$ for complete conversion to cob(II)alamin, only 0.1 equiv of cob(II)alamin is formed. This decrease in formation of the catalytically active radical species at the active site clearly contributes significantly to the reduction of steady-state catalytic activity supported by (α-ribo)AdoCbl. However, there is also a 160-fold decrease in the rate of RTPR-induced carbon−cobalt bond cleavage, corresponding to an increase in the free energy of activation of 3.1 kcal mol^{-1}. This value is slightly smaller than the loss of binding energy (5.1 kcal mol^{-1}) calculated from the steady-state kinetics so that the loss of binding energy normally used to activate the coenzyme could well explain the decrease in the rate of cleavage of the carbon−cobalt bond.

There is considerable evidence from studies of AdoCbl analogues that hydrogen bonding to the Ado ligand is important to the interaction between AdoCbl and its enzymes. In their study of 2′,5′-dideoxyAdoCbl, which has little or no activity with methylmalonyl-CoA mutase [although it has some activity with the less demanding[2] RTPR (*21*)], Calafat et al. (*31*) suggested that the 2′-OH group forms a hydrogen bond with the protein during or after Co−C bond cleavage, thus stabilizing either the transition state or the products of this cleavage. Toraya and co-workers have reported (*26*, *27*) coenzymic activity for A1-deaza- and A3-deaza-AdoCbl with diol dehydrase, but found A7-deaza-AdoCbl and A10-*N*,*N*-dimethyl-AdoCbl to be inactive, competitive inhibitors. A-10-*N*-monomethyl-AdoCbl is also a partially active coenzyme with glycerol dehydrase (*22*). The simplest explanation is that A7 and A10 are essential hydrogen bonding functionalities whose pK_a's (and hence donor and acceptor strengths) are influenced by the atom substitutions at A1 and A3. The question of hydrogen bonding to the Ado moiety of AdoCbl at enzyme active sites clearly needs further investigation, particularly into the effects of atom substitutions and deletions on the structure and three-dimensional conformation of AdoCbl analogues.

Yet another possibility is that at least some of the AdoCbl-requiring enzymes, including RTPR, use mechanical strain to catalyze the cleavage of the carbon−cobalt bond (*3*, *5*−*7*, *72*−*81*). Known as the corrin ring "butterfly" distortion mechanism, or the "mechanochemical trigger" mechanism, this hypothesis includes upward folding of the corrin ring creating strain in the carbon−cobalt bond via steric interactions between the corrin and the Ado ligand. This may result from a steric compression of the axial Co−N bond, causing steric interactions between the bulky Bzm ligand and the corrin ring, which are relieved by upward folding of the corrin (*3*, *75*, *78*, *81*, *82*). Support for this notion comes from the observation that substitution of the much less bulky imidazole for Bzm in CNCbl significantly decreases the corrin ring fold angle (*81*). While a recent X-ray crystal structure of methylmalonyl-CoA mutase (*83*) (which unfortunately failed to locate the Ado ligand of bound coenzyme) and spectroscopic measurements (*84*) showing that the axial Bzm is displaced by a histidine residue in this enzyme makes this mechanism seem less likely for the mutase class of AdoCbl-dependent enzymes, it is now clear that diol dehydrase (*85*) and RTPR bind AdoCbl base-on.

Such compression of the axial Co−C bond would have a large energy cost, but as pointed out above, the intrinsic affinity of cobalamins for proteins is extremely high. The observed binding of AdoCbl to the AdoCbl-dependent enzymes is much weaker, suggesting that substantial binding energy may well be available for compressing the axial Co−N bond. For example, the measured binding constant for AdoCbl binding to RTPR is 5×10^3 M^{-1} (*86*) so that the free energy of binding, ΔG_b, is only −3.1 kcal mol^{-1}. For diol dehydrase, K_m is 0.99 μM (*20*) so that $K_b < 1.0 \times 10^6$ M^{-1} and $-\Delta G_b < 8.2$ kcal mol^{-1}. Thus, considering the 23 kcal mol^{-1} binding energy for CNCbl binding to haptocorrin (*68*), some 15−20 kcal of binding energy could be available for steric compression of the axial Co−N bond in these enzymes.

For (α-ribo)AdoCbl, the corrin ring is "flatter" (i.e., less upwardly folded) than in AdoCbl, although the axial Co−N bond length remains the same. This implies that a greater amount of energy would be needed to increase the upward fold of the corrin, whether by axial Co−N bond compression or otherwise, and sterically strain the Co−C bond. If such a mechanochemical mechanism is indeed operating, this difference in corrin ring fold could then explain the observed loss of binding energy.

Clearly, much remains to be learned about the mechanism (or mechanisms) of enzymatic catalysis of Co−C bond cleavage in AdoCbl. Further studies of the structure and

conformation of active and inactive AdoCbl analogues will be most helpful in this regard.

ACKNOWLEDGMENT

The authors are grateful to Prof. J. Stubbe (Massachusetts Institute of Technology) for the generous gift of *E. coli* HB101/PSQUIRE.

SUPPORTING INFORMATION AVAILABLE

A description of the potential energy functions used in molecular modeling, a description of the water structure and hydrogen bonding in the crystal of (α-ribo)AdoCbl, tables of crystal data and structure refinement, atomic coordinates and equivalent isotropic displacement parameters, bond lengths and angles, anisotropic displacement parameters, hydrogen atom coordinates, and isotropic displacement parameters, an NMR correlation table, tables of ^{1}H and ^{13}C NMR assignments, observed nOe's and nOe intensities, and interproton distances during the 300 ps MD simulation of (α-ribo)AdoCbl, and figures showing an ORTEP diagram of (α-ribo)AdoCbl, a portion of the nucleotide loop of the 27 annealed structures, the flexibility in the C ring of the 27 annealed structures, the observed variability of some of the side chains in the 27 annealed structures, and stopped-flow absorbance traces for the RTPR-induced cleavage of the carbon−cobalt bond of AdoCbl and (α-ribo)AdoCbl (42 pages). Ordering information is given on any current masthead page.

REFERENCES

1. Finke, R. G., and Hay, B. P. (1984) *Inorg. Chem. 23*, 3041.
2. Hay, B. P., and Finke, R. G. (1986) *J. Am. Chem. Soc. 108*, 4820.
3. Hay, B. P., and Finke, R. G. (1987) *J. Am. Chem. Soc. 109*, 8012.
4. Brown, K. L., Cheng, S., Zubkowski, J. D., and Valente, E. J. (1997) *Inorg. Chem. 36*, 1772.
5. Halpern, J. (1985) *Science 227*, 869.
6. Randaccio, L., Bresciani-Pahor, N., Zangrando, E., and Marzilli, L. G. (1989) *Chem. Soc. Rev. 18*, 225.
7. Marzilli, L. G. (1993) in *Bioinorganic Chemistry* (Reedijk, J., Ed.) p 227, Marcel Dekker, New York.
8. Lenhert, P. G. (1968) *Proc. R. Soc. London, Ser. A 303*, 45.
9. Savage, H. F. J., Lindley, P. F., Finney, J. L., and Timmons, P. A. (1987) *Acta Crystallogr. B43*, 280.
10. Savage, H. (1989) *Biophys. J. 50*, 947.
11. Bouquiere, J. P., Finney, J. L., Lehman, M. S., Lindley, P. F., and Savage, H. F. J. (1993) *Acta Crystallogr. B49*, 79.
12. Bouquiere, J. P., Finney, J. L., and Savage, H. F. L. (1994) *Acta Crystallogr. B50*, 566.
13. Bouquiere, J. P. (1992) *Physica B (Amsterdam) 180/181*, 745.
14. Marques, H. M., and Brown, K. L. (1995) *J. Mol. Struct. (THEOCHEM) 340*, 97.
15. Marques, H. M., and Brown, K. L. (1995) *Inorg. Chem. 34*, 3733.
16. Brown, K. L., and Marques, H. M. (1996) *Polyhedron 13*, 2187.
17. Bax, A., Marzilli, L. G., and Summers, M. F. (1987) *J. Am. Chem. Soc. 109*, 566.
18. Morley, C. G. D., Blakley, R. L., and Hogenkamp, H. P. C. (1968) *Biochemistry 7*, 1231.
19. Tamao, T., Morikawa, T., Shimizu, S., and Fukui, S. (1968) *Biochim. Biophys. Acta 151*, 260.
20. Toraya, T., Shirakashi, T., Fukui, S., and Hogenkamp, H. P. C. (1975) *Biochemistry 14*, 3949.
21. Sando, G. N., Blakley, R. L., Hogenkamp, H. P. C., and Hoffman, P. J. (1975) *J. Biol. Chem. 250*, 8774.
22. Yakusheva, M. I., Poznanskaya, A. A., Pospelova, T. A., Rudakova, I. P., Yurkevich, A. M., and Yakovlev, V. A. (1977) *Biochim. Biophys. Acta 484*, 216.
23. Toraya, T., Krodel, E., Mildvan, A. S., and Abeles, R. H. (1979) *Biochemistry 18*, 417.
24. Anton, D. L., Tsai, P. K., and Hogenkamp, H. P. C. (1980) *J. Biol. Chem. 255*, 4507.
25. Toraya, T., and Fukui, S. (1980) *Adv. Chem. Ser. 191*, 139.
26. Ushio, K., Fukui, S., and Toraya, T. (1984) *Biochim. Biophys. Acta 788*, 318.
27. Toraya, T., Matsumoto, T., Ichikawa, M., Itoh, T., Sugawara, T., and Mizuno, Y. (1986) *J. Biol. Chem. 261*, 9289.
28. Toraya, T., and Ishida, A. (1991) *J. Biol. Chem. 266*, 5430.
29. Toraya, T., Miyoshi, S., Mori, M., and Wada, K. (1994) *Biochim. Biophys. Acta 250*, 8774.
30. Poppe, L., Hull, W. E., and Rétey, J. (1993) *Helv. Chim. Acta 76*, 2367.
31. Calafat, A. M., Taoka, S., Puckett, J. M., Semerad, C., Yan, H., Luo, L., Chen, H., Banerjee, R., and Marzilli, L. G. (1995) *Biochemistry 34*, 14125.
32. Brown, K. L., Cheng, S., and Marques, H. M. (1998) *Polyhedron 17*, 2213.
33. Pagano, T. G., Marzilli, L. G., Flocco, M. M., Tsai, C., Carrell, H. L., and Glusker, J. P. (1991) *J. Am. Chem. Soc. 113*, 531.
34. Schramm, G., Lünzmann, G., and Bechmann, F. (1967) *Biochim. Biophys. Acta 145*, 221.
35. Onodera, K., Hirano, S., and Masuda, F. (1967) *Carbohydr. Res. 4*, 263.
36. Furukawa, Y., Imai, K., and Honjo, M. (1968) *Tetrahedron Lett.*, 4655.
37. Dinglinger, F., and Renz, P. (1971) *Hoppe-Zeyler's Z. Physiol. Chem. 352*, 1157.
38. Booker, S., and Stubbe, J. (1993) *Proc. Natl. Acad. Sci. U.S.A. 90*, 8352.
39. Lunn, C. A., Kathju, S., Wallace, C., Kushner, S., and Pigiet, V. (1984) *J. Biol. Chem. 259*, 10468.
40. Russel, R., and Model, P. (1985) *J. Bacteriol. 163*, 238.
41. Blakley, R. L. (1978) *Methods Enzymol. 51*, 246.
42. Licht, S., Gerfen, G. J., and Stubbe, J. (1996) *Science 271*, 477.
43. Sheldrick, G. (1990) *SHELXS-93: A program for the automated solution of crystal structures from X-ray data*, University of Göttingen, Göttingen, Germany.
44. Sheldrick, G. (1997) *SHELXS-97: A program for refinement of crystal structures*, University of Göttingen, Göttingen, Germany.
45. Lai, T. F., and Marsh, R. E. (1972) *Acta Crystallogr. B28*, 1982.
46. Allinger, N. L. (1977) *J. Am. Chem. Soc. 89*, 8127.
47. Clore, G. M., Brünger, A. T., Karplus, M., and Gronenborn, A. M. (1986) *J. Mol. Biol. 191*, 523.
48. Braun, W., Wider, G., Lee, K. H., and Wüthrich, K. (1983) *J. Mol. Biol. 169*, 921.
49. Williamson, M. P., Havel, T. F., and Wüthrich, K. (1985) *J. Mol. Biol. 182*, 295.
50. Clore, G. M., Gronenborn, A. M., Brüger, A. T., and Karplus, M. (1985) *J. Mol. Biol. 185*, 435.
51. Clore, G. M., and Gronenborn, A. M. (1991) *Science 252*, 1390.
52. Allen, M. P., and Tildesley, D. J. (1987) *Computer Simulation of Liquids*, Claredon, Oxford, U.K.
53. Saiz, E., and Tarazona, M. P. (1997) *J. Chem. Educ. 74*, 1350.
54. Berendsen, H. J. C., Postma, J. P. M., van Gunsteren, W. F., DiNola, A., and Haak, J. R. (1984) *J. Chem. Phys. 81*, 3684.
55. Glusker, J. P. (1982) in *B_{12}* (Dolphin, D., Ed.) p 23, Wiley-Interscience, New York.
56. Summers, M. F., Marzilli, L. G., and Bax, A. (1986) *J. Am. Chem. Soc. 108*, 4285.
57. Brown, K. L., Zou, X., Savon, S. R., and Jacobsen, D. W. (1993) *Biochemistry 32*, 8421.
58. Brown, K. L., Zou, X., Wu, G.-D., Zubkowski, J. D., and Valente, E. J. (1995) *Polyhedron 14*, 1621.
59. Brown, K. L., Evans, D. R., Zubkowski, J. D., and Valente, E. J. (1996) *Inorg. Chem. 35*, 415.

60. Sugiyama, H., Yamoaka, N., Shimizu, B., Ishido, Y., and Seto, S. (1974) *Bull. Chem. Soc. Jpn. 47*, 1815.
61. Brown, K. L., Cheng, S., Zou, X., Zubkowski, J. D., Valente, E. J., Knapton, L., and Marques, H. M. (1997) *Inorg. Chem. 36*, 3666.
62. Tamao, Y., and Blakley, R. L. (1973) *Biochemistry 12*, 24.
63. Giessner-Prettre, C., and Pullman, B. (1976) *Biopolymers 15*, 2277.
64. Hoogendorp, J. D., Verschoor, G. C., and Romers, C. (1978) *Acta Crystallogr. B43*, 3662.
65. Brennan, R. G., Kondo, N. S., and Sundaralingam, M. (1984) *J. Am. Chem. Soc. 106*, 5671.
66. Nexø, E., and Olesen, H. (1981) *Biochim. Biophys. Acta 667*, 370.
67. Newmark, P. A., Green, R., Musso, A. M., and Mollin, D. L. (1973) *Br. J. Haematol. 25*, 359.
68. Marchaj, A., Jacobsen, D. W., Savon, S. R., and Brown, K. L. (1995) *J. Am. Chem. Soc. 117*, 11640.
69. Fersht, A. R. (1974) *Proc. R. Soc. London, Ser. B 187*, 397.
70. Firsht, A. R. (1977) *Enzyme Structure and Mechanism*, Chapters 10 and 11, W. H. Freeman, San Francisco.
71. Wilkinson, A. J., Fersht, A. R., Blow, D. M., and Winter, G. (1983) *Biochemistry 22*, 3581.
72. Hill, H. A. O., Pratt, J. M., and Williams, R. J. P. (1969) *Chem. Br. 5*, 156.
73. Chemaly, S. M., and Pratt, J. M. (1980) *J. Chem. Soc., Dalton Trans.*, 2274.
74. Pratt, J. M. (1982) in *B_{12}* (Dolphin, D., Ed.) Vol. 1, p 325, Wiley-Interscience, New York.
75. Bresciani-Pahor, N., Forcolin, M., Marzilli, L. G., Randaccio, L., Summers, M. F., and Toscano, P. J. (1985) *Coord. Chem. Rev. 63*, 1.
76. Rossi, M., Glusker, J. P., Randaccio, L., Summers, M. F., Toscano, P. J., and Marzilli, L. G. (1985) *J. Am. Chem. Soc. 107*, 1729.
77. Pett, V. B., Liebman, M. N., Murray-Rust, P., Prasad, K., and Glusker, J. P. (1987) *J. Am. Chem. Soc. 109*, 3207.
78. Brown, K. L., and Brooks, H. B. (1991) *Inorg. Chem. 30*, 3420.
79. Sagi, I., and Chance, M. R. (1992) *J. Am. Chem. Soc. 114*, 8061.
80. Waddington, M. D., and Finke, R. G. (1993) *J. Am. Chem. Soc. 115*, 4629.
81. Kräutler, B., Konrat, R., Stupperich, E., Fäber, G., Gruber, K., and Kratky, C. (1994) *Inorg. Chem. 33*, 4128.
82. Kräutler, B. (1987) *Helv. Chim. Acta 70*, 1268.
83. Mancia, F., Keep, N. H., Nakagawa, A., Leadley, P. F., McSweeney, S., Rasmussen, B., Bösecke, P., Diat, O., and Evans, P. R. (1996) *Structure 4*, 339.
84. Padmakumar, R., Taoka, S., Padmakumar, R., and Banerjee, R. (1995) *J. Am. Chem. Soc. 117*, 7033.
85. Toraya, T. (1998) in *Vitamin B_{12} and B_{12}-Proteins* (Kräutler, B., Arigoni, D., and Golding, B. T., Eds.) p 303, Wiley-VCH, Weinheim, Germany.
86. Singh, D., Tamao, Y., and Blakely, R. L. (1977) *Adv. Enzyme Regul. 15*, 81.

BI980707M